Article

# Group 10 and 11 Metal Boratranes (Ni, Pd, Pt, CuCl, AgCl, AuCl, and Au) Derived from a Triphosphine#Borane

Marie Sircoglou, Se#bastien Bontemps, Ghenwa Bouhadir, Nathalie Saffon, Karinne Miqueu, Weixing Gu, Maxime Mercy, Chun-Hsing Chen, Bruce M. Foxman, Laurent Maron, Oleg V. Ozerov, and Didier Bourissou

*J. Am. Chem. Soc.*, **2008**, 130 (49), 16729-16738 • DOI: 10.1021/ja8070072 • Publication Date (Web): 13 November 2008



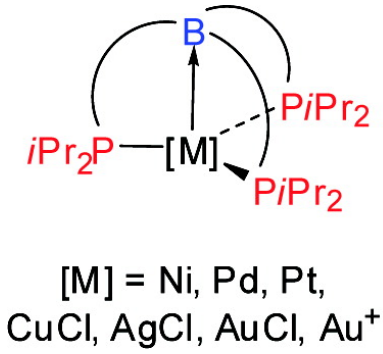


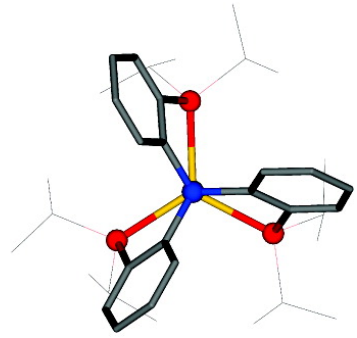

## More About This Article

Additional resources and features associated with this article are available within the HTML version:

- Supporting Information
- Access to high resolution figures
- Links to articles and content related to this article
- Copyright permission to reproduce figures and/or text from this article

View the Full Text HTML

J|A|C|S
ARTICLES

Published on Web 11/13/2008

# Group 10 and 11 Metal Boratranes (Ni, Pd, Pt, CuCl, AgCl, AuCl, and $Au^+$) Derived from a Triphosphine−Borane

Marie Sircoglou,[†] Sébastien Bontemps,[†] Ghenwa Bouhadir,[†] Nathalie Saffon,[‡] Karinne Miqueu,[§] Weixing Gu,[||] Maxime Mercy,[⊥] Chun-Hsing Chen,[||] Bruce M. Foxman,[||] Laurent Maron,*[,⊥] Oleg V. Ozerov,*[,||] and Didier Bourissou*[,†]

*Laboratoire Hétérochimie Fondamentale et Appliquée (UMR−CNRS 5069) and Structure Fédérative Toulousaine en Chimie Moléculaire (FR 2599), Université Paul Sabatier, 118, route de Narbonne, F-31062 Toulouse Cedex 09, France, Institut Pluridisciplinaire de Recherche sur l'Environnement et les Matériaux UMR−CNRS 5254, Equipe "Chimie−Physique", Hélioparc, 2 Avenue du Président Angot, 64053 Pau Cedex 09, France, Department of Chemistry, Brandeis University, MS015, 415 South Street, Waltham, Massachusetts 02454, and the Laboratoire de Physique et Chimie des Nanoobjets (UMR−CNRS 5215), INSA, Université Paul Sabatier, 135, avenue de Rangueil, F-31077 Toulouse Cedex, France*

Received September 4, 2008; E-mail: dbouriss@chimie.ups-tlse.fr

***Abstract:*** The ambiphilic triphosphine−borane ligand **1** {TPB = [*o*-*i*$Pr_2$P-($C_6H_4$)]$_3$B} readily coordinates to all group 10 and 11 metals to afford a complete series of metal boratranes (TPB)[M] **2**−**8** (**2**: M = Ni, **3**: M = Pd, **4**: M = Pt, **5**: M = CuCl, **6**: M = AgCl, **7**: M = AuCl, **8**: M = $Au^+$). Spectroscopic and structural characterization unambiguously establishes the presence of M→B interactions in all of these complexes. The first evidence for borane coordination to copper and silver is provided, and the Au→B interaction is shown to persist upon chloride abstraction. Experimental and theoretical considerations indicate that the M→B interaction is strongest in the Pt and Au complexes. The influence of the oxidation state and charge of the metal is substantiated, and the consequences of relativistic effects are discussed. The coordination of the $\sigma$-acceptor borane ligand is found to induce a significant bathochromic shift of the UV−vis spectra, the Ni, Pd, and Pt complex presenting strong absorptions in the visible range. In addition, all of the group 10 and 11 metal boratranes adopt $C_3$ symmetry both in the solid state and in solution. The central M→B interaction is found to moderately influence the degree of helicity and configurational stability of these three-bladed propellers, and DFT calculations support a dissociative pathway for the inversion process.

## Introduction

Besides the well-known L- and X-type ligands, the ability of Lewis acids to act as $\sigma$-acceptor ligands for transition metals was recognized early on and referred to as Z-type ligands.[1] Although such $\sigma$-acceptor ligands remain considerably much less developed than their $\sigma$-donor counterparts, significant advances have been achieved over the past few years, especially with group 13 Lewis acids $ER_3$ (E = Al, B, etc.).[2−4] In particular, transition metal complexes of boranes, long considered only as putative chemical curiosities,[5,6] have recently been authenticated unambiguously. The first solid-state structure was reported in 1999 by Hill and co-workers for a cage complex **A** [with MLL′ = Ru(CO)($PPh_3$)] (Chart 1).[7] Following this pioneering contribution, hydrido tris(imazolyl)borate ligands proved general precursors for metal boratranes **A** and **B**,[8,9] and M→B interactions were progressively evidenced for all group 8 to group 10 metals.[8−10] Complex **C**,[10] derived from a dihydrido bis(imazolyl)borate derivative, illustrated that the

[†] Laboratoire Hétérochimie Fondamentale et Appliquée.
[‡] Structure Fédérative Toulousaine en Chimie Moléculaire.
[§] Institut Pluridisciplinaire de Recherche sur l'Environnement et les Matériaux.
[⊥] Laboratoire de Physique et Chimie des Nanoobjets.
[||] Brandeis University.

(1) (a) King, R. B. *Adv. Chem. Ser.* **1967**, *62*, 203–220. (b) Green, M. L. H. *J. Organomet. Chem.* **1995**, *500*, 127–148.
(2) Z-type ligands are not restricted to group 13 Lewis acids, as early on exemplified with pyramidal $\eta^1$-$SO_2$ complexes: Kubas, G. J. *Acc. Chem. Res.* **1994**, *27*, 183–190.
(3) For alane and gallane complexes, see: (a) Burlitch, J. M.; Leonowicz, M. E.; Petersen, R. B.; Hughes, R. E. *Inorg. Chem.* **1979**, *18*, 1097–1105. (b) Golden, J. T.; Peterson, T. H.; Holland, P. L.; Bergman, R. G.; Andersen, R. A. *J. Am. Chem. Soc.* **1998**, *120*, 223–224. (c) Braunschweig, H.; Gruss, K.; Radacki, K. *Angew. Chem., Int. Ed.* **2007**, *46*, 7782–7784. (d) Braunschweig, H.; Gruss, K.; Radacki, K. *Inorg. Chem.* **2008**, *47*, 8595–8597.
(4) For recent reviews on TM complexes of boron neutral ambiphilic ligands featuring group 13 Z-type coordination sites, see respectively: (a) Braunschweig, H.; Kollann, C.; Rais, D. *Angew. Chem., Int. Ed.* **2006**, *45*, 5254–5274. (b) Fontaine, F.-G.; Boudreau, J.; Thibault, M.-H. *Eur. J. Inorg. Chem.* DOI: 10.1002/ejic.200800784.
(5) Early claims for transition metal−borane complexes [(a) Shriver, D. F. *J. Am. Chem. Soc.* **1963**, *85*, 3509–3510. (b) Parshall, G. W. *J. Am. Chem. Soc.* **1964**, *86*, 361–364. (c) Johnson, M. P.; Shriver, D. F. *J. Am. Chem. Soc.* **1966**, *88*, 301–304.] were not supported by structural authentication and their real identity has been strongly questioned: (d) Braunschweig, H.; Wagner, T. *Chem. Ber.* **1994**, *127*, 1613–1614. (e) Braunschweig, H.; Wagner, T. *Z. Naturforsch. B* **1996**, *51*, 1618–1620. (f) Braunschweig, H.; Kollann, C. *Z. Naturforsch. B* **1999**, *54*, 839–842.
(6) The borane complex $Et_4N^+[CpFe(CO)_2(BPh_3)]^-$ has been only spectroscopically characterized: Burlitch; J. M.; Burk, J. H.; Leonowicz, M. E.; Hugues, R. E. *Inorg. Chem.* **1979**, *18*, 1702–1709.
(7) Hill, A. F.; Owen, G. R.; White, A. J. P.; Williams, D. J. *Angew. Chem., Int. Ed.* **1999**, *38*, 2759–2761.

  

***Chart 1.*** Structurally Characterized Metal Boratranes **A**−**C**

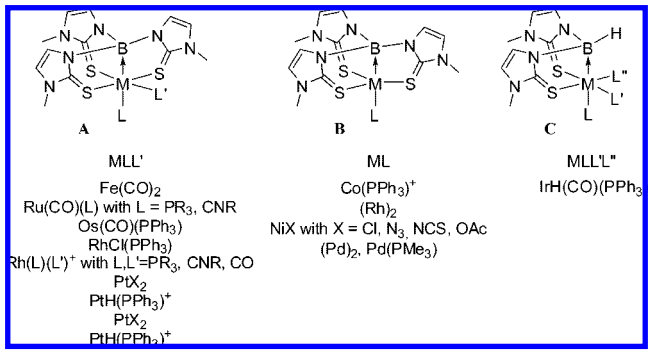


M→B interaction may be supported by only two donor buttresses. Notably, the contribution of the M→B interaction has also been pointed out in the bonding description of boryl metallocenes,[11] borataalkene complexes,[12] and boryl-bridged complexes.[13]

In addition, we have demonstrated that M→B interactions are readily accessible by coordination of so−called ambiphilic ligands combining donor and acceptor coordination sites.[14] Accordingly, the coordination of the diphosphine−borane DPB afforded square pyramidal complexes **I** and **II** free of $\sigma$-donor ligand in the position *trans* to the Lewis acid,[15] as well as square planar complexes **III** (Chart 2).[16] The formation of T-shape

***Chart 2.*** Structurally Characterized Complexes **I**−**V** Derived from Phosphine−Borane Ligands and Featuring M→B Interactions (R = *i*Pr or Ph)

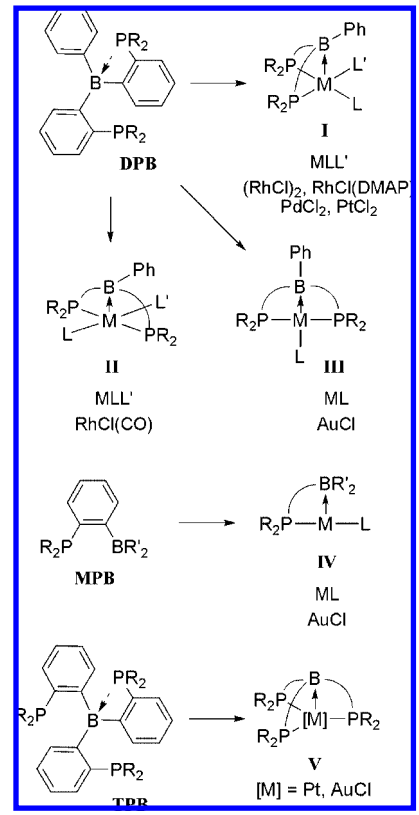


complexes **IV** from the related monophosphine−borane MPB illustrated the possibility for M→B interactions to occur in 14e complexes, even when supported by a single donor buttress.[17] Lastly, the corresponding triphosphine−borane TPB was shown to readily coordinate to Pt and AuCl as a tetradentate $L_3Z$ ligand, affording metal boratranes **V** with intrinsic $C_3$ symmetry.[18]

The coordination of preformed ambiphilic ligands affords straightforward access to transition metal complexes featuring coordinated Lewis acids and thereby facilitates the preparation of a complete series of homologous complexes. Stimulated by the opportunity to extend further the scope of M→B interactions and to gain more insight into the very influence of the metal on their magnitude, we engaged an in-depth study of metal boratranes derived from TPB.[19] Although the cage structure imposed by the tetradentate TPB ligand may minimize the variation of the central M→B interactions, it was expected to facilitate comparisons between group 10 and 11 metal fragments by preventing alternative coordination modes (with the borane remaining pendant[13] or interacting with a chlorine atom at the metal[14i,w,17]). Here we report the synthesis, spectroscopic and structural characterization of the first complete series of complexes with both group 10 and group 11 metals. The first evidence for Cu→B and Ag→B interactions is provided, and the Au→B interaction is shown to persist upon chloride abstraction. Experimental and theoretical considerations indicate that the M→B interaction is strongest in the Pt and Au complexes. The influence of the oxidation state and charge of the metal is substantiated, and the consequences of relativistic effects are discussed. Coordination of the $\sigma$-acceptor borane ligand induces a significant bathochromic shift in the UV−vis spectra, with the Ni, Pd, and Pt complexes presenting strong absorptions in the visible range. In addition, all of the group 10

(8) (a) Foreman, M. R. St.-J.; Hill, A. F.; White, A. J. P.; Williams, D. J. *Organometallics* **2004**, *23*, 913–916. (b) Crossley, I. R.; Hill, A. F. *Organometallics* **2004**, *23*, 5656–5658. (c) Mihalcik, D. J.; White, J. L.; Tanski, J. M.; Zakharov, L. N.; Yap, G. P. A.; Incarvito, C. D.; Rheingold, A. L.; Rabinovitch, D. *Dalton Trans.* **2004**, 1626–1634. (d) Crossley, I. R.; Hill, A. F.; Humphrey, E. R.; Willis, A. C. *Organometallics* **2005**, *24*, 4083–4086. (e) Crossley, I. R.; Foreman, M. R. St.-J.; Hill, A. F.; White, A. J. P.; Williams, D. J. *Chem. Commun.* **2005**, 221–223. (f) Crossley, I. R.; Hill, A. F.; Willis, A. C. *Organometallics* **2006**, *25*, 289–299. (g) Landry, V. K.; Melnick, J. G.; Buccella, D.; Pang, K.; Ulichny, J. C.; Parkin, G. *Inorg. Chem.* **2006**, *45*, 2588–2597. (h) Senda, S.; Ohki, Y.; Hirayama, T.; Toda, D.; Chen, J.-L.; Matsumoto, T.; Kawaguchi, H.; Tatsumi, K. *Inorg. Chem.* **2006**, *45*, 9914–9925. (i) Pang, K.; Quan, S. M.; Parkin, G. *Chem. Commun.* **2006**, 5015–5017. (j) Figueroa, J. S.; Melnick, J. G.; Parkin, G. *Inorg. Chem.* **2006**, *45*, 7056–7058. (k) Hill, A. F. *Organometallics* **2006**, *25*, 4741–4743. (l) Parkin, G. *Organometallics* **2006**, *25*, 4744–4747. (m) Crossley, I. R.; Hill, A. F.; Willis, A. C. *Organometallics* **2007**, *26*, 3891–3895. (n) Crossley, I. R.; Hill, A. F. *Dalton Trans.* **2008**, 201–203. (o) Crossley, I. R.; Hill, A. F.; Willis, A. C. *Organometallics* **2008**, *27*, 312–315. (p) Crossley, I. R.; Foreman, M. R. St.-J.; Hill, A. F.; Owen, G. R.; White, A. J. P.; Williams, D. J.; Willis, A. C *Organometallics* **2008**, *27*, 381–386. (q) Pang, K.; Tanski, J. M.; Parkin, G. *Chem. Commun.* **2008**, 1008–1010.

(9) Connelly et al. have reported a related rhodium boratrane deriving from a hydrido tris(5-thioxo-1,2,4-triazolyl)borate: Blagg, R. J.; Charmant, J. P. H.; Connelly, N. G.; Haddow, M. F.; Orpen, A. G. *Chem. Commun.* **2006**, 2350–2352.

(10) Crossley, I. R.; Hill, A. F.; Willis, A. C. *Organometallics* **2005**, *24*, 1062–1064.

(11) (a) Scheibitz, M.; Bolte, M.; Bats, J. W.; Lerner, H.-W.; Nowik, I.; Herber, R. H.; Krapp, A.; Lein, M.; Holthausen, M. C.; Wagner, M. *Chem. Eur. J.* **2005**, *11*, 584–603. (b) Venkatasubbaiah, K.; Zakharov, L. N.; Kassel, W. S.; Rheingold, A. L.; Jäkle, F. *Angew. Chem., Int. Ed.* **2005**, *44*, 5428–5433, and references therein.

(12) (a) Cook, K. S.; Piers, W. E.; Woo, T. K.; McDonald, R. *Organometallics* **2001**, *20*, 3927–3937. (b) Cook, K. S.; Piers, W. E.; Hayes, P. G.; Parvez, M. *Organometallics* **2002**, *21*, 2422–2425. (c) Cook, K. S.; Piers, W. E.; McDonald, R. *J. Am. Chem. Soc.* **2002**, *124*, 5411–5418.

(13) (a) Curtis, D.; Lesley, M. J. G.; Norman, N. C.; Orpen, A. G.; Starbuck, J. *J. Chem. Soc., Dalton Trans.* **1999**, 1687–1694. (b) Westcott, S. A.; Marder, T. B.; Baker, R. T.; Harlow, R. L.; Calabrese, J. C.; Lam, K. C.; Lin, Z. *Polyhedron* **2004**, *23*, 2665–2677. (c) Braunschweig, H.; Radacki, K.; Rais, D.; Whittell, G. R. *Angew. Chem., Int. Ed.* **2005**, *44*, 1192–1193.

***Scheme 1.*** Synthesis of Group 10 Metal Boratranes **2**−**4**

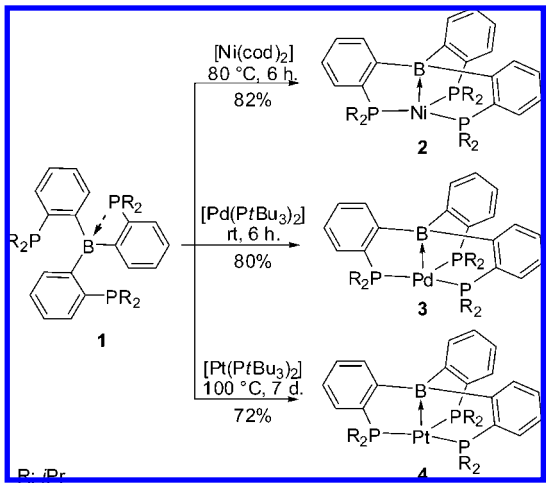


and 11 metal boratranes adopt $C_3$ symmetry both in the solid state and in solution. The central M→B interaction is found to moderately influence the degree of helicity and configurational stability of these three-bladed propellers, and DFT calculations support a dissociative pathway for the inversion process.

## Results

**Synthesis and Characterization of Group 10 Metal Boratranes.** The nickel boratrane **2**was readily obtained by reacting the triphosphine−borane **1**[20] with [Ni(cod)$_2$] at 80 °C in toluene for 6 h (Scheme 1). After removal of the volatiles and washing with pentane, complex **2** was isolated in 82% yield.[21] The dark blue color of **2** is associated with a strong absorption at $\lambda_{max} = 572$ nm in its UV−vis spectrum (in toluene solution). The unique signal observed at $\delta = 35.0$ ppm in the $^{31}$P NMR spectrum of **2** is consistent with symmetric coordination of the three phosphorus atoms, while the high-field $^{11}$B NMR chemical shift ($\delta = 15.9$ ppm) strongly suggests the presence of a dative Ni→B interaction.[22] X-ray quality crystals of **2** (monoclinic, space group *Cc*) were obtained from a toluene/pentane solution at −35 °C (Figure 1, Table 4). The overall structure of **2** strongly resembles that of the related platinum boratrane **4**,[18] with the metal center adopting a trigonal monopyramidal geometry and only slightly deviating from the basal plane formed by the three phosphorus atoms (0.103 Å in **2**). The boron atom is in a strongly pyramidal environment (sum of the CBC bond angles $\Sigma B_\alpha = 339.1°$) diagnostic for a M→B interaction. The NiB bond length (2.1677(16) Å) is slightly longer than that found by Tatsumi and Parkin in nickel(I) boratranes featuring tris(imazolyl)borane ligands (2.08−2.11 Å).[8h,q]

The geometry of complex **2** only marginally deviates from $C_3$ symmetry, and its helicity, as quantified by the average P−M−B−C torsion angle $\theta$,[23] amounts to 26.2°. In line with these solid-state observations, two signals attributable to the *exo*/*endo* $CH(CH_3)_2$ moieties were observed in both the $^1$H and $^{13}$C NMR spectra of **2**. According to variable-temperature $^1$H NMR experiments, the coalescence temperature slightly exceeds 100 °C. The energy barrier for the inversion of the helical structure can thus be estimated to slightly exceed 17.3(±0.5) kcal/mol.[21]

The related palladium boratrane **3** was prepared following the same route as that used for its platinum analog **4**.[18] The sterically hindered phosphines of [Pd(P*t*Bu$_3$)$_2$] were displaced by the triphosphine−borane **1** under mild conditions (6 h at room temperature). After workup, complex **3** was isolated in 80% yield as a red powder.[21] Its UV−vis spectrum in toluene solution displays a strong absorption at 511 nm. The $^{31}$P NMR spectrum of **3** exhibits a single resonance (at $\delta = 41.3$ ppm), and the presence of a dative Pd→B interaction is supported by a high-field $^{11}$B NMR chemical shift ($\delta = 27.3$ ppm). The metal boratrane structure of **3** was unambiguously established by X-ray crystallography (triclinic crystals, space group $P\bar{1}$) (Figure 2, Table 4). The axial PdB bond (2.2535(17) Å) is longer than

(14) For PB, PAl, and NB systems, see: (a) Labinger, J. A.; Miller, J. S. *J. Am. Chem. Soc.* **1982**, *104*, 6856–6858. (b) Grimmett, D. L.; Labinger, J. A.; Bonfiglio, J. N.; Masuo, S. T.; Shearin, E.; Miller, J. S. *J. Am. Chem. Soc.* **1982**, *104*, 6858–6859. (c) Labinger, J. A.; Bonfiglio, J. N.; Grimmett, D. L.; Masuo, S. T.; Shearin, E.; Miller, J. S. *Organometallics* **1983**, *2*, 733–740. (d) Yuan, Z.; Taylor, N. J.; Marder, T. B.; Williams, I. D.; Kurtz, S. K.; Cheng, L.-T. *Chem. Commun.* **1990**, 1489–1492. (e) Yuan, Z.; Taylor, N. J.; Sun, Y.; Marder, T. B.; Williams, I. D.; Cheng, L.-T. *J. Organomet. Chem.* **1993**, *449*, 27–37. (f) Braunschweig, H.; Dirk, R.; Ganter, B. *J. Organomet. Chem.* **1997**, *545*−*546*, 257–266. (g) Fontaine, F.-G.; Zargarian, D. *J. Am. Chem. Soc.* **2004**, *126*, 8786–8794. (h) Emslie, D. J. H.; Blackwell, J. M.; Britten, J. F.; Harrington, L. E. *Organometallics* **2006**, *25*, 2412–2414. (i) Oakley, S. R.; Parker, K. D.; Emslie, D. J. H.; Vargas-Baca, I.; Robertson, C. M.; Harrington, L. E.; Britten, J. F. *Organometallics* **2006**, *25*, 5835–5838. (j) Welch, G. C.; San Juan, R. R.; Masuda, J. D.; Stephan, D. W. *Science* **2006**, *314*, 1124–1126. (k) Thibault, M.-H.; Boudreau, J.; Mathiotte, S.; Drouin, F.; Sigouin, O.; Michaud, A.; Fontaine, F.-G. *Organometallics* **2007**, *26*, 3807–3815. (l) Bebbington, M. W. P.; Bouhadir, G.; Bourissou, D. *Eur. J. Org. Chem.* **2007**, 4483–4486. (m) Vergnaud, J.; Ayed, T.; Hussein, K.; Vendier, L.; Grellier, M.; Bouhadir, G.; Barthelat, J.-C.; Sabo-Etienne, S.; Bourissou, D. *Dalton Trans.* **2007**, 2370–2372. (n) Chase, P. A.; Welch, G. C.; Jurca, T.; Stephan, D. W. *Angew. Chem., Int. Ed.* **2007**, *46*, 8050–8053. (o) Spies, P.; Erker, G.; Kehr, G.; Bergander, K.; Fröhlich, R.; Grimme, S.; Stephan, D. W. *Chem. Commun.* **2007**, 5072–5074. (p) Welch, G. C.; Cabrera, L.; Chase, P. A.; Hollink, E.; Masuda, J. D.; Wei, P.; Stephan, D. W. *Dalton Trans.* **2007**, 3407–3414. (q) Thangavelu, S. G.; Hocker, K. E.; Cooke, S. R.; Muhoro, C. N. *J. Organomet. Chem.* **2008**, *693*, 562–566. (r) Fischbach, A.; Bazinet, P. R.; Waterman, R.; Tilley, T. D. *Organometallics* **2008**, *27*, 1135–1139. (s) Vergnaud, J.; Grellier, M.; Bouhadir, G.; Vendier, L.; Sabo-Etienne, S.; Bourissou, D. *Organometallics* **2008**, *27*, 1140–1146. (t) Sircoglou, M.; Bouhadir, G.; Saffon, N.; Miqueu, K.; Bourissou, D. *Organometallics* **2008**, *27*, 1675–1678. (u) Chikkali, S.; Magens, S.; Gudat, D.; Nieger, M.; Hartenbach, I.; Schleid, T. *Eur. J. Inorg. Chem.* **2008**, 2207–2213. (v) Miller, A. J. M.; Labinger, J. A.; Bercaw, J. E. *J. Am. Chem. Soc.* **2008**, *130*, 11874–11875. (w) Emslie, D. J. H.; Harrington, L. E.; Jenkins, H. A.; Robertson, C. M.; Britten, J. F. *Organometallics* **2008**, *27*, 5317–5325.

(15) (a) Bontemps, S.; Gornitzka, H.; Bouhadir, G.; Miqueu, K.; Bourissou, D. *Angew. Chem., Int. Ed.* **2006**, *45*, 1611–1614. (b) Bontemps, S.; Sircoglou, M.; Bouhadir, G.; Puschmann, H.; Howard, J. A. K.; Dyer, P. W.; Miqueu, K.; Bourissou, D. *Chem. Eur. J.* **2008**, *14*, 731–740.

(16) Sircoglou, M.; Bontemps, S.; Mercy, M.; Saffon, N.; Takahashi, M.; Bouhadir, G.; Maron, L.; Bourissou, D. *Angew. Chem., Int. Ed.* **2007**, *46*, 8583–8586.

(17) Bontemps, S.; Bouhadir, G.; Miqueu, K.; Bourissou, D. *J. Am. Chem. Soc.* **2006**, *128*, 12056–12057.

(18) Bontemps, S.; Bouhadir, G.; Gu, W.; Mercy, M.; Chen, C.-H.; Foxman, B. M.; Maron, L.; Ozerov, O. V.; Bourissou, D. *Angew. Chem., Int. Ed.* **2008**, *47*, 1481–1484.

(19) The essentially pure $\sigma$-donor character of the phosphine buttresses (compared with the $\sigma$- and $\pi$-basic character of imazolyl ligands) allows for a clear unambiguous focus on $\sigma$-effects in the complexes deriving from TPB.

(20) Bontemps, S.; Bouhadir, G.; Dyer, P. W.; Miqueu, K.; Bourissou, D. *Inorg. Chem.* **2007**, *46*, 5149–5151.

(21) See Supporting Information.

(22) Transition metal complexes of phosphine−boranes featuring M→B interactions typically display $^{11}$B NMR chemical shifts from 18 to 55 ppm,[15−18] while tris(imazolyl)-based metal boratranes display values closer to 0 ppm.[8,9]

(23) This parameter has been introduced to quantify the chiral twist in $C_3$-symmetric complexes of hydrotris(imazolyl)borate ligands: Foreman, M. R. St.-J.; Hill, A. F.; White, A. J. P.; Williams, D. J. *Organometallics* **2003**, *22*, 3831–3840.

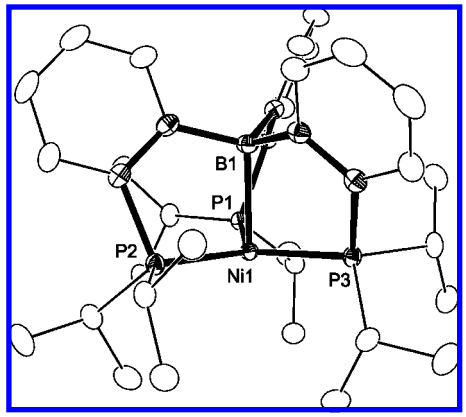


***Figure 1.*** Molecular view of the nickel boratrane **2** in the solid state, with hydrogen atoms omitted.

those found in related tris(imazolyl)borane Pd complexes (2.05−2.07 Å)[8i] but is appreciably shorter than that observed in the (DPB)$PdCl_2$ complex (2.650(3) Å).[15b] The pronounced pyramidalization of the boron environment ($\Sigma B_\alpha = 341.8°$) further substantiates the presence of a Pd→B interaction in **3**.

The palladium boratrane **3** displays $C_3$ symmetry in the solid state, with the three PCCBPd metallacycles adopting envelope conformations oriented in the same direction (average torsion angle $\theta = 28.3°$). Here also, the *exo*/*endo* environments for the $CH(CH_3)_2$ groups were distinguished by $^1$H and $^{13}$C NMR spectroscopy, and the inversion barrier of the three-blade propeller, as deduced from variable-temperature NMR experiments, amounts to 15.6(±0.5) kcal/mol for **3**.[21]

**Synthesis and Characterization of Group 11 Metal Boratranes.** The copper and silver boratranes **5** and **6** were prepared by adding 1 equiv of the triphosphine−borane **1** to a suspension of the corresponding metal(I) chloride in dichloromethane (Scheme 2). In both cases, the reaction mixture immediately became homogeneous, and for copper, the solution turned yellow. After standard workup, complexes **5** and **6** were obtained in 75% and 90% yield, respectively.[21] The UV−vis spectrum of the copper complex **5** in toluene solution displays two absorptions at 343 and 404 nm. The $^{31}$P NMR spectrum of **5** displays a unique signal at $\delta\ ^{31}P = 18.8$ ppm, in agreement with the symmetric coordination of the three phosphorus atoms. The $^{31}$P NMR spectrum of **6** exhibits a pair of doublets of almost equal intensity centered at $\delta = 26.2$ ppm. The coupling constants with the two silver isotopes are well-resolved [$^1J(^{109}Ag,^{31}P) =$ 300 Hz and $^1J(^{107}Ag,^{31}P) = 259$ Hz] and consistent with the

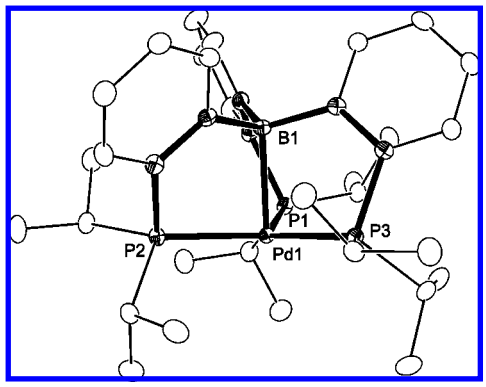


***Figure 2.*** Molecular view of the palladium boratrane **3** in the solid state, with hydrogen atoms omitted.

***Scheme 2.*** Synthesis of Group 11 Metal Boratranes **5**−**8**

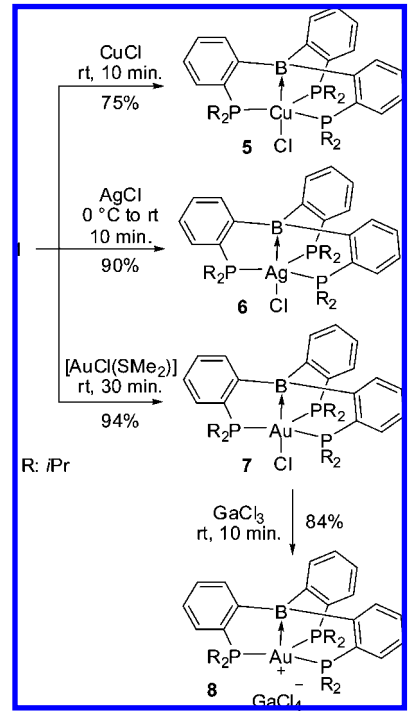


$^{109}$Ag/$^{107}$Ag gyromagnetic ratio. The $^{11}$B NMR chemical shift of 53.8 ppm observed for both **5** and **6** is significantly lower than that expected for a free triarylborane ($\delta\ ^{11}$B ∼70 ppm),[24] and very similar to those observed in (DPB)$PtCl_2$ and (DPB)-$PdCl_2$ complexes,[15b] suggesting the presence of weak M→B interactions. To gain greater insight into the precise structure of these group 11 metal boratranes, single crystals suitable for X-ray diffraction analyses were obtained from saturated dichloromethane solutions at low temperature (Figures 3 and 4, Table 4). In both complexes, the metal center is pentacoordinate and adopts a trigonal-bipyramidal geometry. The boron and chlorine atoms define the apical axis, while the three phosphorus atoms occupy the basal positions. The CuCl (2.367(1) Å) and AgCl (2.580(1) Å) bond lengths are at the upper limit of those reported for related borane-free tris(phosphine)complexes.[25] The CuB (2.508(2) Å) and AgB (2.540(2) Å) bond lengths are significantly longer than that found in the related gold boratrane **7** (2.318(8) Å)[18] but still appreciably shorter than the sum of the van der Waals radii (3.8 Å for CuB and 3.9 Å for AgB).[26] Along with the noticeable pyramidalization of the boron environment ($\Sigma B_\alpha = 347.0°$ in **5** and 347.4° in **6**), this supports the presence of M→B interactions, and to the best of our knowledge, complexes **5** and **6** provide the first examples of borane coordination to copper and silver.[27,28]

As their heavier analog **7**, the copper and silver boratranes **5** and **6** display $C_3$ symmetry (trigonal crystals, space group $R\bar{3}$),

(24) (a) Brown, N. M. D.; Davidson, F.; Wilson, J. W. *J. Organomet. Chem.* **1981**, *209*, 1–11. (b) Brown, H. C.; Racherla, U. S. *J. Org. Chem.* **1986**, *51*, 427–432.
(25) According to Cambridge Database searches, the CuCl (resp. AgCl) bond length in tris(phosphine) complexes range from 2.28 to 2.38 Å (resp. 2.47 to 2.59 Å).
(26) Batsanov, S. S. *Inorg. Mater.* **2001**, *37*, 871–885.
(27) Nagashima et al. recently evidenced the presence of dative Cu→Zr interactions within the heterobimetallic complexes [ClZr(RNPPh$_2$)$_3$ CuCl] (R = *t*Bu, *i*Pr): Sue, T.; Sunada, Y.; Nagashima, H. *Eur. J. Inorg. Chem.* **2007**, 2897–2908.

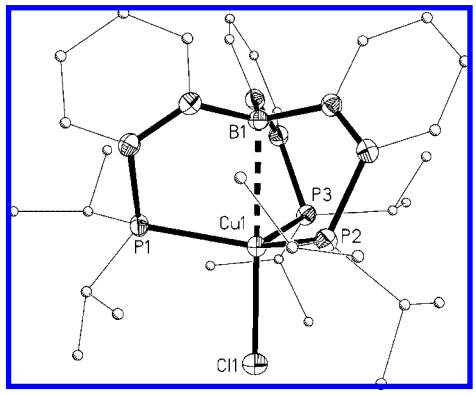


***Figure 3.*** Molecular view of the copper boratrane **5** in the solid state, with hydrogen atoms and solvate molecules omitted.

with helicity parameters $\theta$ of 29.4° and 29.8°, respectively. According to $^{1}$H and $^{13}$C NMR spectroscopy, both complexes retain this three-bladed propeller geometry in solution, and as previously, variable-temperature experiments allowed estimation of their inversion barriers [16.1(±0.5) kcal/mol for **5** and 17.1(±0.5) kcal/mol for **6**].[21]

The neutral/cationic charge of the metal center, as well as the presence or the absence of a $\sigma$-donor ligand *trans* to B, can be anticipated to influence the magnitude of M→B interactions. In this perspective, we then prepared the cationic gold boratrane **8**. Chloride abstraction from the neutral complex **7** was readily achieved with gallium(III) chloride in dichloromethane at room temperature. After standard workup, complex **8** was isolated in 84% yield as a pale yellow powder. Upon cationization, the $^{31}$P NMR resonance is shifted to lower field by about 20 ppm (from $\delta$ $^{31}$P = 47.6 ppm in **7**, to 70.0 ppm in **8**). At the same time, the $^{11}$B NMR signal is deshielded by about 30 ppm (from $\delta$ $^{11}$B = 27.7 ppm in **7**, to 56.6 ppm in **8**), suggesting an appreciable weakening of the Au→B interaction. This was confirmed by X-ray crystallography (Figure 5, Table 4). The shortest contact between (TPB)$Au^{+}$ and $GaCl_4^{-}$ (3.003 Å between a hydrogen atom of a methyl group and a chlorine atom) unambiguously established the ion pair character of **8**. The tetracoordinate gold center adopts a trigonal-monopyramidal geometry. Upon cationization, the AuB bond is elongated (from 2.318(8) Å in **7**,[18] to 2.448(8) Å in **8**) but remains noticeably shorter than the sum of the van der Waals radii (3.9 Å).[26] In the same time, the pyramidalization of the boron environment decreases (from $\Sigma B_\alpha$ = 339.3° in **7**,[18] to 351.3° in **8**). All of these data suggest that the cationic boratrane **8** retains some Au→B interaction, albeit significantly weakened compared to that of its neutral precursor **7**.

The $C_3$ symmetry of the metal boratrane structure is also retained upon cationization, and the degree of helicity is almost

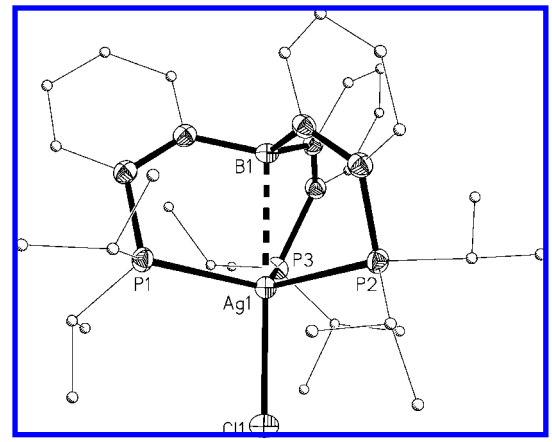


***Figure 4.*** Molecular view of the silver boratrane **6** in the solid state, with hydrogen atoms and solvate molecules omitted.

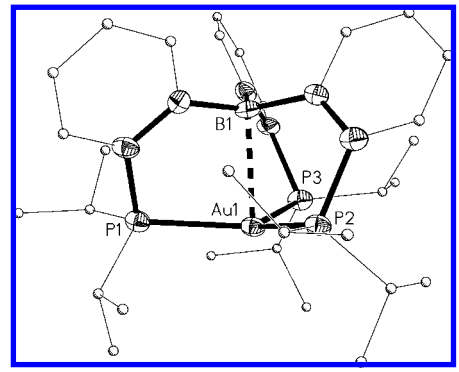


***Figure 5.*** Molecular view of the cationic gold boratrane **8** in the solid state, with hydrogen atoms, solvate molecules, and counteranion omitted.

unchanged (from $\theta$ = 27.0° in **7**,[18] to 28.4° in **8**). According to $^{1}$H and $^{13}$C NMR spectroscopy, the neutral and cationic gold boratranes exhibit very similar characteristics in solution, and the barriers predicted by variable-temperature experiments for the inversion of the helical structure are identical [14.9(±0.5) kcal/mol for **8** vs 14.7(±0.5) kcal/mol for **7**].[21]

## Discussion

**Group 10 Metal Boratranes.** For the sake of comparison, the main data concerning the (TPB)M complexes **2**−**4** (M = Ni, Pd, Pt) are collected in Table 1. From a geometric viewpoint, the MB bond lengths fall within a rather narrow range (from 2.17 Å with Ni, to 2.22 Å with Pt, and 2.25 Å with Pd). In order to take into account the different sizes of the metals involved, these MB distances were compared with the sum of covalent atomic radii that have been recently revisited by S. Alvarez et al. (Figure 6).[29] Accordingly, the ratio $r$ = d(M-B)/$\Sigma(R_{cov})$ only marginally exceeds 1 for all complexes (from 1.01 with Pd and Pt, to 1.04 with Ni). This supports the presence of a rather strong M→B interaction in all of these metal boratranes. However, the MB bond length alone cannot be considered a reliable parameter to compare the magnitude of these M→B interactions within group 10, especially in such cage structures. Thus, a set of complementary parameters were considered.

(28) For recent experimental and theoretical investigations on boryl complexes of group 11 metals, see: (a) Laitar, D. S.; Müller, P.; Sadighi, J. P. *J. Am. Chem. Soc.* **2005**, *127*, 17196–17197. (b) Laitar, D. S.; Tsui, E. Y.; Sadighi, J. P. *J. Am. Chem. Soc.* **2006**, *128*, 11036–11037. (c) Zhao, H.; Lin, Z.; Marder, T. B. *J. Am. Chem. Soc.* **2006**, *128*, 15637–15643. (d) Lillo, V.; Fructos, M. R.; Ramírez, J.; Braga, A. A. C.; Maseras, F.; Díaz-Requejo, M. M.; Pérez, P. J.; Fernández, E. *Chem. Eur. J.* **2007**, *13*, 2614–2621. (e) Dang, L.; Zhao, H.; Lin, Z.; Marder, T. B. *Organometallics* **2007**, *26*, 2824–2832. (f) Segawa, Y.; Yamashita, M.; Nozaki, K. *Angew. Chem., Int. Ed.* **2007**, *46*, 6710–6713. (g) Dang, L.; Zhao, H.; Lin, Z.; Marder, T. B. *Organometallics* **2008**, *27*, 1178–1186. (h) Dang, L.; Zhao, H.; Lin, Z.; Marder, T. B. *J. Am. Chem. Soc.* **2008**, *130*, 5586–5594. (i) Dang, L.; Lin, Z.; Marder, T. B. *Organometallics* **2008**, *27*, 4443–4454.

(29) Cordero, B.; Gómez, V.; Pletro-Prats, A. E.; Revés, M.; Echeverría, J.; Cremades, E.; Barragán, F.; Alvarez, S. *Dalton Trans.* **2008**, 2832–2838.

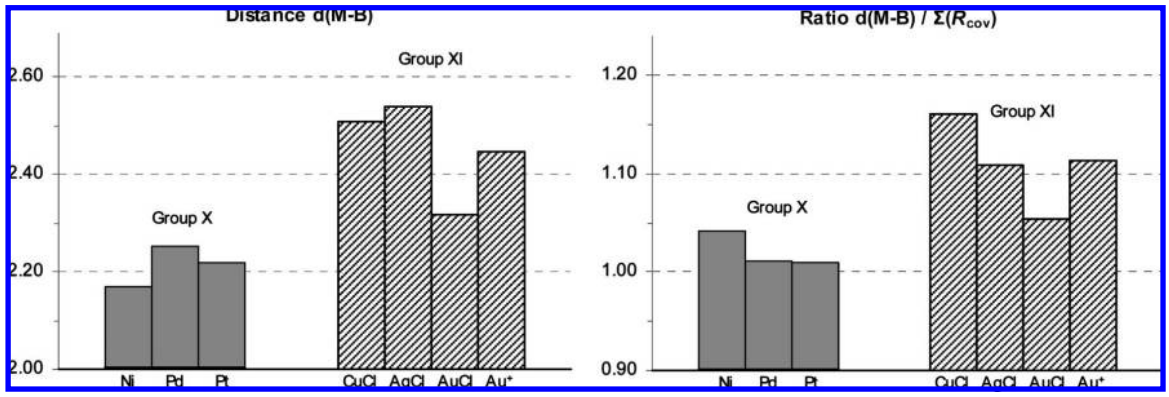


***Figure 6.*** Influence of the metal on the MB distance [$d$(M−B) in Å], as determined crystallographically, in the group 10 and 11 series. $\Sigma(R_{cov})$ was calculated from the set of covalent atomic radii recently revisited by S. Alvarez.[29]

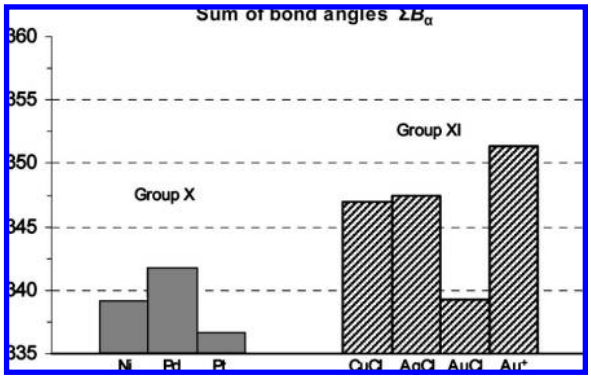


***Figure 7.*** Variation of the pyramidalization of the boron environment ($\Sigma B_\alpha$ in deg), as determined crystallographically, with the nature of the metal in the group 10 and 11 series.

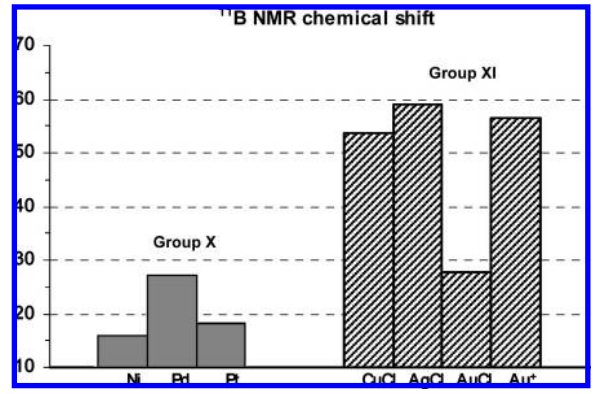


***Figure 8.*** Variation of the $^{11}$B NMR chemical shift (in ppm), as determined experimentally, with the nature of the metal in the group 10 and 11 series.

The pyramidalization of the boron environment also proved useful to estimate the degree of M→B interaction.[15b] In all of the metal boratranes **2**−**4**, the geometry around boron strongly deviates from planarity, with $\Sigma B_\alpha$ ranging from 336° to 342° (Figure 7). The slight decrease of $\Sigma B_\alpha$ from Pd (341.8°) to Ni (339.1°) and Pt (336.7°) suggests some strengthening of the M→B interaction that culminates with platinum.

The $^{11}$B NMR chemical shift can also be considered an interesting spectroscopic probe for the interaction of boranes with Lewis bases. In this perspective, the values found for **2**−**4** are in the lower range of those reported so far for metal→borane complexes,[15−18] which further supports the presence of strong M→B interactions in the group 10 metal boratranes (Figure 8). In addition, the slightly higher $^{11}$B NMR chemical shift obtained for the Pd complex **3** (27.3 ppm compared with 18.2 ppm for the Pt complex **4**, and with 15.9 ppm for the Ni complex **2**) suggests that the Pd→B interaction would be somewhat weaker than Pt→B and Ni→B interactions.

To shed more light into the M→B interactions involved in metal boratranes **2**−**4**, DFT calculations were carried out on the actual complexes at the B3PW91/SDD(Ni,Pd,Pt,P),6-31G**(B,C,H) level of theory.[21] The optimized geometries fit closely with those determined experimentally (largest deviation of only 0.03 Å for the MB bond length), confirming the capability of the method in describing such complexes. The $^{11}$B NMR chemical shifts of complexes **2**−**4** were computed via the Gauge Including Atomic Orbitals (GIAO) method. The calculated values exceed the measured ones by about 5−6 ppm, but the experimental trend was nicely reproduced, the maximal value of $\delta^{11}$B, tentatively associated with the weaker M→B interaction, being predicted for the palladium boratrane **3** (Table 1).

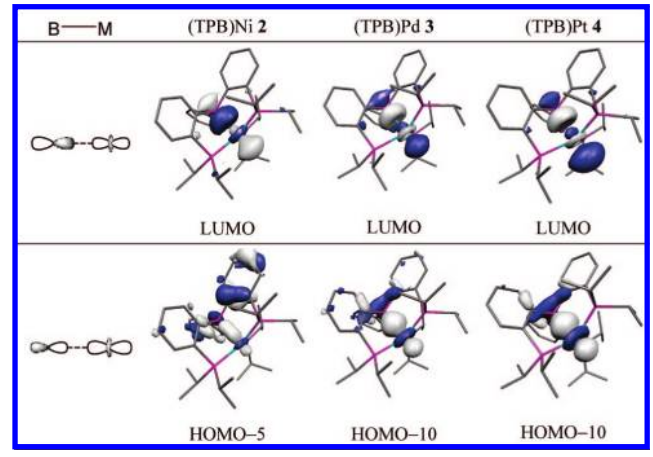


***Figure 9.*** Molecular orbital plots associated with the 2e−2c BM interaction within group 10 metal boratranes **2**−**4**.

Analysis of the molecular orbitals of **2**−**4** indicated two-center, two-electron bonding interactions between the metal center and the borane moiety (Figure 9). For each group 10 metal boratrane, the LUMO corresponds to an antibonding combination of the $d_{z^2}$ (M) and 2p(B) orbitals, whose bonding counterpart is associated with the HOMO−5 (with Ni) or HOMO−10 (with Pd and Pt).

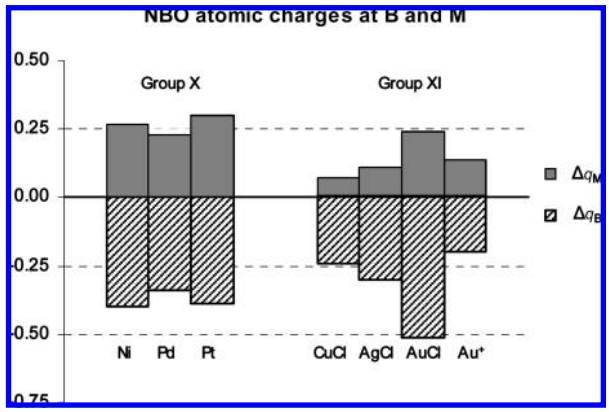


***Figure 10.*** Variation of the NBO atomic charges at B and M, as calculated from $\Delta q_B = q_B$ (complex) $- q_B$ (free TPB ligand, open form) and $\Delta q_M = q_M$ (TPB complex) $- q_M$ (borane-free complex).

***Table 1.*** Geometric Data (Bond Lengths and Angles in Å and deg, Respectively), $^{11}$B NMR Chemical Shifts ($\delta$ $^{11}$B in ppm, Relative to $BF_3 \cdot OEt_2$), NBO Atomic Charges ($\Delta q_B$ and $\Delta q_M$), NBO Stabilizing Energies Associated with the M→B Interaction ($\Delta E_{int.}$ in kcal/mol) and UV-vis Absorptions ($\lambda_{max}$ in nm) Determined Experimentally and/or Computed at the B3PW91/SDD(Ni,Pd,Pt,P),6-31G**(other atoms) Level of Theory for Group 10 Metal Boratranes **2**−**4**

| | (TPB)Ni **2** | | (TPB)Pd **3** | | (TPB)Pt **4** | |
|---|---|---|---|---|---|---|
| | exptl | DFT | exptl | DFT | exptl | DFT |
| MB | 2.168 | 2.164 | 2.254 | 2.248 | 2.220 | 2.246 |
| av MP | 2.199 | 2.266 | 2.349 | 2.406 | 2.296 | 2.376 |
| $\Sigma B_\alpha$ | 339.1 | 341.2 | 341.8 | 340.5 | 336.7 | 338.4 |
| av $\theta^a$ | 26.2 | 29.7 | 28.3 | 28.8 | 24.3 | 27.0 |
| $\delta$ $^{11}$B | +15.9 | +22.8 | +27.3 | +31.8 | +18.2 | +24.5 |
| $\Delta q_B{}^b$ | | −0.40 | | −0.34 | | −0.39 |
| $\Delta q_M{}^c$ | | +0.27 | | +0.23 | | +0.30 |
| $\Delta E_{int}{}^d$ | | 61.2 | | 64.6 | | 145.1 |
| $\lambda_{max}$ | 572 | 549[e] | 511 | 501<br>511 | 541 | 519<br>528 |

[a] Average P−M−B−C torsion angle. [b] $\Delta q_B = q_B$ (complex) $- q_B$ (free TPB ligand, open form). [c] $\Delta q_M = q_M$ (TPB complex) $- q_M$ (borane-free complex). [d] Associated with the main M→B donor−acceptor interaction found at the second order. [e] Associated with two degenerated transitions.

The atomic charges at the boron and metal centers, derived from NBO analyses of **2**−**4**, provided further insight into the influence of the metal. The amount of electron transfer from the metal to the boron was estimated via (i) the difference $\Delta q_B$ between the charge at boron in the metal boratrane complex (TPB)M and that in the free ligand TPB in its open form[30] and (ii) the difference $\Delta q_M$ between the charge at the metal in the metal boratrane complex (TPB)M and that in the related boron-free complex M(P*i*Pr$_2$Ph)$_3$ (Figure 10). As anticipated, the donor−acceptor M→B interaction resulted in negative values of $\Delta q_B$ and positive values of $\Delta q_M$. The weaker variations were found with palladium (**3**: $\Delta q_B = -0.34$, $\Delta q_M = +0.23$), and quasi-identical values were obtained with nickel (**2**: $\Delta q_B = -0.40$, $\Delta q_M = +0.27$) and platinum (**4**: $\Delta q_B = -0.39$, $\Delta q_M = +0.30$). This supports that the M→B interaction would be somewhat stronger with Pt and Ni than with Pd, in line with the trend deduced from the $^{11}$B NMR chemical shift and the sum of bond angles $\Sigma B_\alpha$.

For all of the complexes **2**−**4**, second-order perturbative NBO analyses revealed the presence of donor−acceptor interactions between the metal and the boron centers. The corresponding delocalization energies $\Delta E_{int}$ (from 60−65 kcal/mol with Ni and Pd to 145 kcal/mol with Pt) fall in the upper range of those observed so far for metal→borane complexes.[31] This suggests further the presence of rather strong M→B interactions in all group 10 metal boratranes **2**−**4** and suggests that platinum forms the strongest such interaction.

(30) TPB **1** exists in solution as a mixture of "closed" and "open" forms (i.e., with or without intramolecular P→B interaction).[20]

***Table 2.*** Geometric Data (Bond Lengths and Angles in Å and deg, Respectively), $^{11}$B NMR Chemical Shifts ($\delta$ $^{11}$B in ppm, Relative to $BF_3 \cdot OEt_2$), NBO Atomic Charges ($\Delta q_B$ and $\Delta q_M$), and NBO Stabilizing Energies Associated with the M→B Interaction ($\Delta E_{int}$ in kcal/mol) Determined Experimentally and/or Computed at the B3PW91/SDD(Cu,Ag,Au,P,Cl),6-31G**(other atoms) Level of Theory for Group 11 Metal Boratranes **5**−**8**

| | (TPB)CuCl **5** | | (TPB)AgCl **6** | | (TPB)AuCl **7** | | (TPB)Au$^+$ **8** | |
|---|---|---|---|---|---|---|---|---|
| | exptl | DFT | exptl | DFT | exptl | DFT | exptl | DFT |
| MB | 2.508 | 2.570 | 2.540 | 2.540 | 2.318 | 2.324 | 2.448 | 2.485 |
| MCl | 2.367 | 2.364 | 2.580 | 2.559 | 2.607 | 2.603 | | |
| av MP | 2.358 | 2.398 | 2.499 | 2.539 | 2.424 | 2.480 | 2.390 | 2.470 |
| $\Sigma B_\alpha$ | 347.0 | 347.5 | 347.4 | 346.1 | 339.3 | 338.6 | 351.3 | 350.8 |
| av $\theta^a$ | 29.40 | 30.70 | 29.80 | 31.03 | 27.00 | 28.57 | 28.37 | 29.00 |
| $\delta$ $^{11}$B | +53.8 | +58.0 | +59.1 | +54.9 | +27.7 | +32.5 | +56.6 | +57.0 |
| $\Delta q_B{}^b$ | | −0.24 | | −0.30 | | −0.51 | | −0.20 |
| $\Delta q_M{}^c$ | | +0.07 | | +0.11 | | +0.24 | | +0.14 |
| $\Delta E_{int}{}^d$ | | 7.9 | | 14.3 | | 46.9 | | 26.5 |

[a] Average P−M−B−C torsion angle. [b] $\Delta q_B = q_B$ (complex) $- q_B$ (free TPB ligand, open form). [c] $\Delta q_M = q_M$ (TPB complex) $- q_M$ (borane-free complex). [d] Associated with the main M→B donor−acceptor interaction found at the second order.

The different parameters used to compare the isoelectronic series of metal boratranes **2**−**4** overall support a nonregular variation among group 10, Pd forming a slightly weaker M→B interaction than Ni and Pt.[32] This most probably results from a complex combination of geometric and electronic effects. Due to its smaller size compared to Pd and Pt, Ni may better fit in the cage structure induced by the tetradentate TPB ligand. On the other hand, the increase of the Lewis basicity of transition metals going down a group[33] is consistent with the fact that the strongest M→B interaction is found with Pt.[34]

Lastly, the optical properties of complexes **2**−**4** were assessed by simulating their UV spectra via time-dependent DFT calculations.[21] In order to gain more insight into the influence of the borane, similar calculations were carried out on the boron-free complexes. The highest wavelength of maximum absorbance predicted for complexes M(P*i*Pr$_2$Ph)$_3$ was found at $\lambda_{max}$ = 422 nm for Ni, whereas absorptions of noticeable intensities were found in the range 500−550 nm for all metal boratranes (Table 1). The values computed for **2**−**4** match well those measured experimentally in toluene (maximum deviation of 23 nm in $\lambda_{max}$). All these absorptions in the visible region are associated with allowed transitions from metal-centered occupied orbitals to the boron-centered LUMO orbital. For each metal boratrane of the group 10 series, this acceptor orbital is readily

(31) NBO calculations deleting the identified M→B interaction led to energy contributions of 59 kcal mol$^{-1}$ (Ni), 51 kcal mol$^{-1}$ (Pd), and 139 kcal mol$^{-1}$ (Pt).

(32) A similar trend (3d,5d > 4d) is observed in $\pi$-backdonation within carbonyl complexes: Hocking, R. K.; Hambley, T. W *Organometallics* **2007**, *26*, 2815–2823.

(33) (a) Shriver, D. F. *Acc. Chem. Res.* **1970**, *3*, 231–238. (b) Angelici, R. J. *Acc. Chem. Res.* **1995**, *28*, 51–60.

(34) Pd is known to form boryl complexes significantly less stable than those with Pt: (a) Braunschweig, H.; Radacki, K.; Rais, D.; Schneider, A.; Seeler, F. *J. Am. Chem. Soc.* **2007**, *129*, 10350–10351. (b) Braunschweig, H.; Gruss, K.; Radacki, K.; Uttinger, K. *Eur. J. Inorg. Chem.* **2008**, 1462–1466.

***Table 3.*** Free Energies of Activation (in kcal/mol) for the Inversion of the Three-Bladed Propeller Structure of Complexes **2**−**8**, as Estimated from $^{1}$H and $^{13}$C NMR Variable-Temperature Experiments[a]

| | (TPB)Ni **2** | (TPB)Pd **3** | (TPB)Pt **4** | (TPB)CuCl **5** | (TPB)AgCl **6** | (TPB)AuCl **7** | (TPB)Au$^{+}$ **8** |
|---|---|---|---|---|---|---|---|
| | | | $^{1}$H NMR | | | | |
| $T_c$ (K) | ≥373 | 333 | | 353 | 373 | 321 | 323 |
| $\Delta\nu$ (Hz) | 257 | 144 | no splitting | 430 | 360 | 303 | 252 |
| $\Delta G^{\ddagger b}$ | ≥17.3 | 15.7 | | 16.0 | 17.0 | 14.7 | 14.9 |
| | | | $^{13}$C NMR | | | | |
| $T_c$ (K) | | 323 | 335 | 330 | 363 | 305 | |
| $\Delta\nu$ (Hz) | coalescence not reached | 89 | 663 | 58 | 137 | 72 | not performed |
| $\Delta G^{\ddagger b}$ | | 15.5 | 14.8 | 16.2 | 17.2 | 14.8 | |

[a] The NMR experiments were performed in toluene-$d_8$ for **2**, **3**, **4**, and **7** and in bromobenzene-$d_5$ for **5**, **6**, and **8**. [b] Calculated via the following formula: $\Delta G^{\ddagger} = RT_c \ln[RT_c\sqrt{2}/(\pi N_A h|\Delta\nu|)]$ with $R$ (gas constant), $T_c$ (coalescence temperature), $N_A$ (Avogadro's number), $h$ (Planck's constant), and $\Delta\nu$ (chemical shift difference).

***Table 4.*** Crystallographic Data for Metal Boratranes **2**, **3**, **5**, **6**, and **8**

| | **2** | **3** | **5** | **6** | **8** |
|---|---|---|---|---|---|
| empirical formula | $C_{43}H_{62}BNiP_3$ | $C_{36}H_{54}BP_3Pd$ | $C_{39}H_{60}BCl_7CuP_3$ | $C_{39}H_{60}AgBCl_7P_3$ | $C_{37}H_{56}AuBCl_6GaP_3$ |
| formula weight | 741.41 | 696.96 | 944.28 | 988.61 | 1083.92 |
| crystal system | monoclinic | triclinic | trigonal | trigonal | triclinic |
| space group | *Cc* | $P\bar{1}$ | $R\bar{3}$ | $R\bar{3}$ | $P\bar{1}$ |
| *a*, Å | 10.8577(3) | 11.0591(5) | 17.7510(4) | 17.8985(4) | 11.1685(10) |
| *b*, Å | 19.0236(6) | 11.2426(6) | 17.7510(4) | 17.8985(4) | 14.4053(14) |
| *c*, Å | 20.0634(6) | 16.7043(8) | 25.1600(12) | 25.1626(11) | 15.9131(14) |
| α, deg | 90 | 76.909(2) | 90 | 90 | 81.638(2) |
| *β*, deg | 104.999(2) | 78.583(2) | 90 | 90 | 70.938(2) |
| *γ*, deg | 90 | 60.716(2) | 120 | 120 | 68.797(2) |
| *V*, Å$^3$ | 4003.0(2) | 1755.10(15) | 6865.7(4) | 6981.0(4) | 2254.9(4) |
| *Z* | 4 | 2 | 6 | 6 | 2 |
| density calcd, Mg.m$^{-3}$ | 1.230 | 1.319 | 1.370 | 1.411 | 1.596 |
| absorp coeff, mm$^{-1}$ | 0.634 | 0.689 | 1.018 | 0.965 | 4.334 |
| reflections collected | 38147 | 51474 | 23149 | 21221 | 11420 |
| independent reflections | 10535 | 9169 | 4264 | 3825 | 7541 |
| refined parameters | 434 | 371 | 177 | 177 | 519 |
| *R*1 ($I > 2\sigma(I)$) | 0.0261 | 0.0327 | 0.0252 | 0.0199 | 0.0483 |
| *wR*2 (all data) | 0.0618 | 0.0882 | 0.0691 | 0.0531 | 0.1213 |
| $(\Delta/r)_{max}$ (e Å$^{-3}$) | 0.54 and −0.55 | −0.49 and 0.71 | 0.433 and −0.283 | 0.391 and −0.283 | 3.782 and −2.394 |

accessible in energy, which explains the large bathochromic shift observed compared with the boron-free complexes.

**Group 11 Metal Boratranes.** Table 2 summarizes the main data concerning the (TPB)MCl complexes **5**−**7** (M = Cu, Ag, Au) and (TPB)Au$^{+}$ complex **8**. The MB bond lengths within the neutral group 11 complexes **5**−**7** vary in a much larger range (from 2.32 Å with Au to 2.51 Å with Cu and 2.54 Å with Ag) than for group 10. As mentioned above, reliable comparison require to take into account the relative size of the metals and thus to consider the ratios $r = d(\text{M}-\text{B})/\Sigma(R_{cov})$. Accordingly, the MB bond length was found to only slightly exceed the sum of covalent atomic radii in the gold complex **7** ($r = 1.05$), and to progressively elongate in the related silver ($r = 1.11$) and copper ($r = 1.16$) complexes **6** and **5**, respectively (Figure 6). The variation of the pyramidalization around boron parallels that of the MB bond length, the sum of bond angles $\Sigma B_\alpha$ increasing from 339.3° with Au to about 347° with both Cu and Ag (Figure 7). The geometric data of group 11 metal boratranes support the presence of M→B interactions with increasing strength from copper and silver to gold. This trend was also apparent spectroscopically, the $^{11}$B NMR chemical shift increasing from 27.7 ppm for the gold complex **7** to 53.8 and 59.1 ppm for the copper and silver complexes **5** and **6**, respectively (Figure 8).

Additional data were obtained by DFT calculations at the B3PW91/SDD(Cu,Ag,Au,P,Cl),6-31G**(B,C,H) level of theory.[21] For each complex **5**−**7**, the optimized structure corresponds closely to the geometry determined crystallographically (largest deviations of only 0.06 Å for the MB bond length, and 1.3° for the sum of bond angles $\Sigma B_\alpha$), further confirming the capability of the method in describing M→B interactions. The calculated $^{11}$B NMR chemical shifts also match well those determined experimentally ($\Delta\delta \pm 5$ ppm). Thus, the trend observed experimentally among group 11 metals was reproduced theoretically, from both the geometric and the spectroscopic viewpoints.

Compared with the group 10 metal boratranes, the presence of the chlorine atom *trans* to boron in the group 11 complexes **5**−**7** results in three-center, four-electron BMCl interactions. The contribution of the 2p(B), $d_{z^2}$ (M), and 3p(Cl) to the corresponding molecular orbitals (Figure 11) significantly deviates from the prototypical case (three identical atomic orbitals), with non-negligible contribution of $d_{z^2}$ (M) in $\Psi_2$ (bonding with B and antibonding with Cl) and essentially M-Cl bonding interaction in $\Psi_1$ and M-B antibonding interaction in $\Psi_3$.

In addition, the computed NBO atomic charges revealed a progressive increase in the electron transfer from the metal to the boron going down the group, with correlated decrease of $\Delta q_B$ (from −0.24 with Cu to −0.30 with Ag and −0.51 with Au) and increase of $\Delta q_M$ (from +0.07 with Cu to +0.11 with Ag and +0.24 with Au). The progressive strengthening of the M→B interaction going down group 11 was further corroborated by second-order pertubative NBO analyses (the delocalization energies $\Delta E_{int}$ associated with the main M→B donor−acceptor

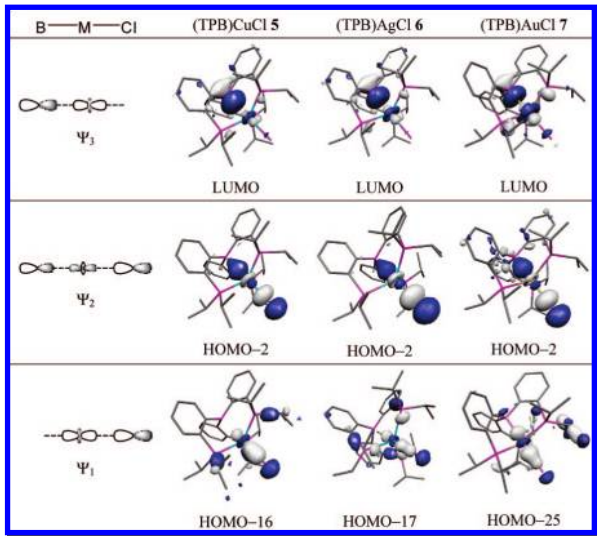


***Figure 11.*** Molecular orbitals associated with the 4e−3c BMCl interactions within the (TPB)MCl group 11 metal boratranes **5**−**7**.

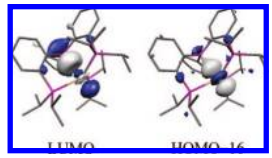

***Figure 12.*** Molecular orbitals associated with the 2e−2c BAu interaction within the (TPB)$Au^+$ complex **8**.

interaction were found to increase from 8 kcal/mol with Cu to 14 kcal/mol with Ag and 47 kcal/mol with Au).[35]

All parameters indicate a progressive strengthening of M→B interactions within complexes **5**−**7** when going down group 11. This variation parallels that of the intrinsic basicity of the metal,[33] and culminates with gold, for which the 5d orbitals are significantly destabilized by relativistic effects.[36,37] As a result, the energy separation between the occupied metal-centered and the vacant boron-centered orbitals decreases, and the magnitude of the M→B interaction increases.[38]

Comparison of the neutral gold boratrane **7** with its cationic analog **8** obtained by chlorine abstraction gives more insight into the influence of the charge of the metal center and of the presence of a $\sigma$-donor coligand in the position *trans* to the Lewis acid. The AuB bond significantly elongates upon cationization (from 2.32 Å in **7** to 2.45 Å in **8**), suggesting a noticeable weakening of the Au→B interaction. This was confirmed by the increase of the sum of bond angles $\Sigma B_\alpha$ (351.8°) and of the $^{11}$B NMR chemical shift (56.6 ppm), which both fall in the same range as those observed for the copper and silver boratranes **5** and **6**. The DFT calculations performed on the actual complex reproduced these geometric and spectroscopic variations and further corroborated the retention of a weakened Au→B interaction in **8**. Indeed, the presence of a two-center, two-electron AuB interaction was apparent from the molecular orbitals (Figure 12), and the NBO atomic charge indicated a transfer of about 0.2 e to the boron atom ($\Delta q_B = -0.20$ for **8** vs −0.51 for **7**). In addition, the delocalization energy $\Delta E_{int}$ associated with the Au→B interaction at the second-order NBO analysis is about half of that predicted for the corresponding neutral complex (26 kcal/mol for **8** vs 47 kcal/mol for **7**).[39]

As observed with group 10 metals, the UV−vis spectra computed for (TPB)MCl complexes **5**−**7** and (TPB)$Au^+$ complex **8** revealed strong bathochromic shifts compared to the related boron-free complexes MCl(P*i*$Pr_2$Ph)$_3$ and Au(P*i*$Pr_2$Ph)$_3^+$. The transitions predicted for the group 11 metal boratranes remain essentially in the UV region, in agreement with their colorless to pale yellow appearance. The highest $\lambda_{max}$ computed was found at 436 nm for (TPB)CuCl **5** (associated with degenerated HOMO−1→LUMO and HOMO→LUMO transitions), in good agreement with the value determined experimentally (404 nm in toluene).[21]

The characterization of the complete series of metal boratranes **2**−**8** makes it possible to illustrate the influence of the metal oxidation state on the magnitude of M→B interactions. As expected, the stronger M→B interactions are found with the metals of lower oxidation state. The variation is rather pronounced for the Ni/Cu and Pd/Ag dyads but much less significant for the Pt/Au dyad, the higher oxidation state of the gold complex being somewhat compensated for by the greater relativistic effects.

**Intrinsic $C_3$ Symmetry of Group 10 and 11 Metal Boratranes.** All metal boratranes **2**−**8** were found to adopt $C_3$ symmetry both in the solid state and in solution. This illustrates the propensity of the Z-type ligand to support chiral three-bladed propeller geometry around transition-metal centers[40] and extends thereby the variety of *intrinsically* $C_3$-symmetric complexes.[41] The helical geometry results from the tendency of the PCCBM metallacycles to adopt envelope conformations and markedly contrasts with the approximately $C_{3v}$ symmetry displayed by the related trigonal bipyramidal metal boratranes **B** deriving from tris(imazolyl)borane ligands (the SCNBM metallacycles typically adopting a planar arrangement).[8c,h,i,q]

From a quantitative viewpoint, the degree of helicity (as deduced crystallographically from the mean value of $\theta$) and the energy barrier for the inversion of the three-bladed propeller $\Delta G^{\ddagger}$ (as estimated spectroscopically by $^1$H and $^{13}$C NMR variable-temperature experiments, Table 3) were found to vary moderately with the nature and strength of the axial M→B interaction ($\theta$ ranges from 25° to 30°, and $\Delta G^{\ddagger}$ ranges from 15 to 17.5 kcal/mol).

(35) NBO calculations deleting the identified M→B interaction led to energy contributions of 3.5 kcal mol$^{-1}$ (CuCl), 7 kcal mol$^{-1}$ (AgCl) and 48.5 kcal mol$^{-1}$ (AuCl).

(36) For recent reviews on gold chemistry, see: (a) Pyykkö, P. *Angew. Chem., Int. Ed.* **2004**, *43*, 4412–4456. (b) Schmidbaur, H.; Cronje, S.; Djordjevic, B.; Schuster, O. *Chem. Phys.* **2005**, *311*, 151–161.

(37) The relativistic effects on valence-shell properties increase roughly like $Z^2$, in which $Z$ is the full nuclear charge.

(38) Similarly, the destabilization of 5d orbitals by the relativistic contraction of the inner orbitals was shown to be responsible for the increased $\pi$-backdonation in $(OC)_5W{=}CH_2$ compared to the related Cr and Mo complexes: Jacobsen, H.; Ziegler, T. *Inorg. Chem.* **1996**, *35*, 775–783.

(39) NBO calculations deleting the Au→B interaction led to an energy contribution of 31 kcal mol$^{-1}$.

(40) For leading reviews, see: (a) Keyes, M. C.; Tolman, W. B. *Adv. Catal. Processes* **1997**, *2*, 189–219. (b) Moberg, C. *Angew. Chem., Int. Ed.* **1998**, *37*, 248–268. (c) Gibson, S. E.; Castaldi, M. P. *Chem. Commun.* **2006**, 3045–3062. (d) Gade, L. H.; Bellemin-Laponnaz, S. *Chem. Eur. J.* **2008**, *14*, 4142–4152.

(41) For representative examples of intrinsically $C_3$-symmetric complexes deriving from $L_3X$-type triphosphine ligands, see: (a) Siclosi, M.; Llort, J.; Estevan, F.; Lahuerta, P.; Sanau, M.; Pérez-Prieto, J. *Angew. Chem., Int. Ed.* **2006**, *45*, 6741–6744. (b) Mankad, N. P.; Whited, M. T.; Peters, J. C. *Angew. Chem., Int. Ed.* **2007**, *46*, 5768–5771.

As discussed by Hill[23] and Bailey[42] for complexes deriving from hydrotris(imazolyl) borate, the inversion of such metal-centered helical cages may proceed via a dissociative or a nondissociative pathway. To gain more insight into the mechanism of inversion involved in metal boratranes (TPB)[M], the nickel and gold boratranes **2** and **7** were selected because they present the largest difference in $\Delta G^{\ddagger}$. No energy extremum could be located on their potential energy surfaces for the corresponding $C_{3v}$ structures that are probably disfavored by an important steric congestion between the isopropyl substituents at neighboring phosphorus atoms. In contrast, dissociation of a phosphine arm was found to be readily accessible in energy (20.3 and 14.8 kcal/mol for Ni and AuCl, respectively). The resulting $\kappa^3$-(TPB)[M] complexes retain short MB contacts (NiB 2.17 Å and AuB 2.37 Å), and their inversions proceed with low barriers (3.0 and 5.0 kcal/mol for Ni and AuCl, respectively). The overall barriers for the inversion of the $C_3$ symmetric (TPB)Ni and (TPB)AuCl complexes were thereby estimated to be 23.3 and 19.8 kcal/mol, respectively. These values correlate reasonably well with those determined experimentally and reproduce the relative stability of the two propeller structures (Ni > AuCl).

## Conclusion

In summary, an in-depth study on metal boratranes has been undertaken by coordination of a triphosphine−borane. A complete series of complexes with group 10 and 11 metals have been prepared and fully characterized in solution and in the crystalline state. Geometric constraints associated with the cage structures complicate the interpretation of the structural and spectroscopic parameters in terms of the strength of the M→B interaction. However, combination of the computational and experimental insight allowed for the consistent analysis of the bonding. Accordingly, Cu→B and Ag→B interactions were evidenced for the first time, and Pt and Au were shown to form stronger M→B interactions than their lighter analogs. In addition, the coordination of the $\sigma$-acceptor borane ligand was found to induce a significant bathochromic shift of the UV−vis spectra. Lastly, all of the group 10 and 11 metal boratranes exhibit intrinsic $C_3$ symmetry. The central M→B interaction was found to moderately influence the degree of helicity and configurational stability of these three-bladed propellers, and DFT calculations support a dissociative pathway for the inversion process.

These results further emphasize the ability of group 13 Lewis acids to behave as $\sigma$-acceptor ligands toward transition metals and thereby to signicantly influence their geometric, stereochemical, and electronic features. In this respect, Z-type ligands should be considered as valuable complements to the extensively used L- and X-type $\sigma$-donor ligands in order to finely tune the properties of transition metal complexes.

**Acknowledgment.** The CNRS, UPS, and ANR programs (project BILI) are warmly acknowledged for financial support of this work. Dr. Y. Coppel (Toulouse, France) is acknowledged for his assistance in the VTP NMR experiments. L.M. thanks CalMip (CNRS, Toulouse, France) and CiNES (CNRS, Montpellier, France) for calculation facilities and the Institut Universitaire de France. We are also grateful for the support of this research by the NSF (CHE-0517798 to OVO and CHE-0521047 to B.M.F. for the diffractometer purchase), the Department of Energy (DE-FG02-86ER13615), the Sloan Foundation, the Dreyfus Foundation, and the Petroleum Research Fund. Drs. Sara Kunz and Christos Douvris are acknowledged for their assistance with $^{11}$B NMR experiments.

**Supporting Information Available:** Experimental and computational details; spectroscopic and X-ray crystallographic data for metal boratranes **2**, **3**, **5**, **6**, and **8** including CIF files; Cartesian coordinates for the optimized structures. This material is available free of charge via the Internet at http://pubs.acs.org.

JA8070072

(42) Bailey, P. J.; Dawson, A.; McCormack, C.; Moggach, S. A.; Oswald, I. D. H.; Parsons, S.; Rankin, D. W. H.; Turner, A. *Inorg. Chem.* **2005**, *44*, 8884–8898.